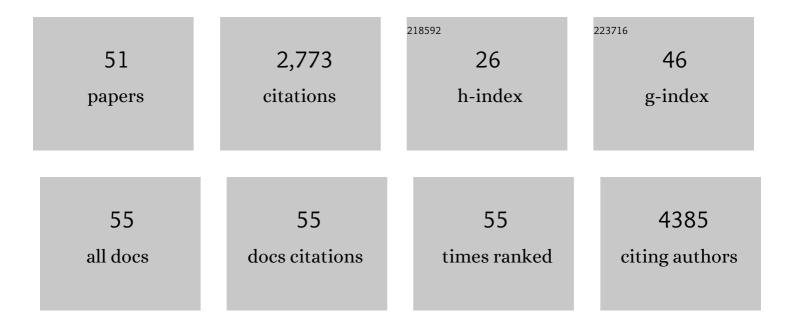
Rui Tang

List of Publications by Year in descending order

Source: https://exaly.com/author-pdf/3704647/publications.pdf Version: 2024-02-01



#	Article	IF	CITATIONS
1	Sulforaphane activates anti-inflammatory microglia, modulating stress resilience associated with BDNF transcription. Acta Pharmacologica Sinica, 2022, 43, 829-839.	2.8	17
2	Tryptophan fluorescence and machine learning to study the aggressiveness of prostate cancer cell lines: A pilot study. , 2022, , 173-183.		1
3	Analysis of Stable Chelate-free Gadolinium Loaded Titanium Dioxide Nanoparticles for MRI-Guided Radionuclide Stimulated Cancer Treatment. Current Analytical Chemistry, 2022, 18, 826-835.	0.6	1
4	Non-invasive monitoring of arthritis treatment response via targeting of tyrosine-phosphorylated annexin A2 in chondrocytes. Arthritis Research and Therapy, 2021, 23, 265.	1.6	0
5	Reduced Nhe1 (Na ⁺ -H ⁺ Exchanger-1) Function Protects ApoE-Deficient Mice From Ang II (Angiotensin II)–Induced Abdominal Aortic Aneurysms. Hypertension, 2020, 76, 87-100.	1.3	7
6	Selective imaging of solid tumours via the calcium-dependent high-affinity binding of a cyclic octapeptide to phosphorylated Annexin A2. Nature Biomedical Engineering, 2020, 4, 298-313.	11.6	31
7	Effects of core titanium crystal dimension and crystal phase on ROS generation and tumour accumulation of transferrin coated titanium dioxide nanoaggregates. RSC Advances, 2020, 10, 23759-23766.	1.7	6
8	Osteotropic Radiolabeled Nanophotosensitizer for Imaging and Treating Multiple Myeloma. ACS Nano, 2020, 14, 4255-4264.	7.3	26
9	Ultrabright fluorescent nanoscale labels for the femtomolar detection of analytes with standard bioassays. Nature Biomedical Engineering, 2020, 4, 518-530.	11.6	110
10	Na+-H+ exchanger 1 determines atherosclerotic lesion acidification and promotes atherogenesis. Nature Communications, 2019, 10, 3978.	5.8	25
11	Trafficking of a Single Photosensitizing Molecule to Different Intracellular Organelles Demonstrates Effective Hydroxyl Radical-Mediated Photodynamic Therapy in the Endoplasmic Reticulum. Bioconjugate Chemistry, 2019, 30, 1451-1458.	1.8	6
12	Electrospray Functionalization of Titanium Dioxide Nanoparticles with Transferrin for Cerenkov Radiation Induced Cancer Therapy. ACS Applied Bio Materials, 2019, 2, 1141-1147.	2.3	16
13	3D Printing of Poloxamer 407 Nanogel Discs and Their Applications in Adjuvant Ovarian Cancer Therapy. Molecular Pharmaceutics, 2019, 16, 552-560.	2.3	34
14	Shape-Dependent Biodistribution of Biocompatible Silk Microcapsules. ACS Applied Materials & Interfaces, 2019, 11, 5499-5508.	4.0	27
15	Perfusionâ€based fluorescence imaging method delineates diverse organs and identifies multifocal tumors using generic nearâ€infrared molecular probes. Journal of Biophotonics, 2018, 11, e201700232.	1.1	6
16	Ultrasmall visible-to-near-infrared emitting silver-sulfide quantum dots for cancer detection and imaging. , 2018, , .		2
17	Bolus injections of novel thrombogenic site-targeted fusion proteins comprising annexin-V and Kunitz protease inhibitors attenuate intimal hyperplasia after balloon angioplasty. International Journal of Cardiology, 2017, 240, 339-346.	0.8	4
18	Nanophotosensitive drugs for light-based cancer therapy: what does the future hold?. Nanomedicine, 2017, 12, 1101-1105.	1.7	14

Rui Tang

#	Article	IF	CITATIONS
19	Augmented reality navigation in open surgery for hilar cholangiocarcinoma resection with hemihepatectomy using video-based in situ three-dimensional anatomical modeling. Medicine (United) Tj ETQq1	1 0.7 8431	l4 3g BT /Ove
20	Novel Injury Site Targeted Fusion Protein Comprising Annexin V and Kunitz Inhibitor Domains Ameliorates Ischemia-Reperfusion Injury and Promotes Survival of Ischemic Rat Abdominal Skin Flaps. Annals of Plastic Surgery, 2017, 78, S129-S134.	0.5	6
21	Proof-of-Concept of Polymeric Sol-Gels in Multi-Drug Delivery and Intraoperative Image-Guided Surgery for Peritoneal Ovarian Cancer. Pharmaceutical Research, 2016, 33, 2298-2306.	1.7	17
22	Tunable Ultrasmall Visible-to-Extended Near-Infrared Emitting Silver Sulfide Quantum Dots for Integrin-Targeted Cancer Imaging. ACS Nano, 2015, 9, 220-230.	7.3	187
23	Protonation and Trapping of a Small pH-Sensitive Near-Infrared Fluorescent Molecule in the Acidic Tumor Environment Delineate Diverse Tumors in Vivo. Molecular Pharmaceutics, 2015, 12, 4237-4246.	2.3	31
24	Probing Distanceâ€Đependent Plasmonâ€Enhanced Nearâ€Infrared Fluorescence Using Polyelectrolyte Multilayers as Dielectric Spacers. Angewandte Chemie - International Edition, 2014, 53, 866-870.	7.2	75
25	Ultrabright NIR fluorescent mesoporous silica nanoparticles. Journal of Materials Chemistry B, 2014, 2, 3107-3114.	2.9	45
26	Synthesis of dye conjugates to visualize the cancer cells using fluorescence microscopy. Applied Optics, 2014, 53, 2345.	0.9	29
27	Native fluorescence spectroscopy reveals spectral differences among prostate cancer cell lines with different risk levels. Journal of Biomedical Optics, 2013, 18, 087002.	1.4	38
28	Pyrazoleâ€substituted Nearâ€infrared Cyanine Dyes Exhibit <scp>pH</scp> â€dependent Fluorescence Lifetime Properties. Photochemistry and Photobiology, 2013, 89, 326-331.	1.3	23
29	Synthesize dye-bioconjugates to visualize cancer cells using fluorescence microscopy. Proceedings of SPIE, 2013, , .	0.8	0
30	Near-infrared fluorescence goggle system with complementary metal–oxide–semiconductor imaging sensor and see-through display. Journal of Biomedical Optics, 2013, 18, 101303.	1.4	50
31	Dual fluorescent molecular substrates selectively report the activation, sustainability and reversibility of cellular PKB/Akt activity. Scientific Reports, 2013, 3, 1697.	1.6	9
32	All-near-infrared multiphoton microscopy interrogates intact tissues at deeper imaging depths than conventional single- and two-photon near-infrared excitation microscopes. Journal of Biomedical Optics, 2013, 18, 106012.	1.4	22
33	Investigation of native fluorescence spectral difference among prostate cancer cell lines with different risk levels. , 2013, , .		Ο
34	Induction of pH Sensitivity on the Fluorescence Lifetime of Quantum Dots by NIR Fluorescent Dyes. Journal of the American Chemical Society, 2012, 134, 4545-4548.	6.6	83
35	Bound 1D Excitons in Single CdSe Quantum Wires. Journal of Physical Chemistry Letters, 2012, 3, 2627-2632.	2.1	14
36	Near-Infrared pH-Activatable Fluorescent Probes for Imaging Primary and Metastatic Breast Tumors. Bioconjugate Chemistry, 2011, 22, 777-784.	1.8	179

Rui Tang

#	Article	IF	CITATIONS
37	Immediate Repair of Major Abdominal Wall Defect After Extensive Tumor Excision in Patients With Abdominal Wall Neoplasm: A Prospective Review of 27 Cases. Annals of Surgical Oncology, 2009, 16, 2895-2907.	0.7	30
38	Exciton localization and migration in individual CdSe quantum wires at low temperatures. Physical Review B, 2009, 80, .	1.1	23
39	Spectroscopic Identification of Tri- <i>n</i> -octylphosphine Oxide (TOPO) Impurities and Elucidation of Their Roles in Cadmium Selenide Quantum-Wire Growth. Journal of the American Chemical Society, 2009, 131, 4983-4994.	6.6	140
40	Size- and Shape-Controlled Synthesis of Bismuth Nanoparticles. Chemistry of Materials, 2008, 20, 3656-3662.	3.2	150
41	The Trouble with TOPO; Identification of Adventitious Impurities Beneficial to the Growth of Cadmium Selenide Quantum Dots, Rods, and Wires. Nano Letters, 2008, 8, 3521-3524.	4.5	166
42	Synchronous Photoluminescence Intermittency (Blinking) along Whole Semiconductor Quantum Wires. Nano Letters, 2007, 7, 3290-3295.	4.5	74
43	Solution-Based Growth and Structural Characterization of Homo- and Heterobranched Semiconductor Nanowires. Journal of the American Chemical Society, 2007, 129, 12254-12262.	6.6	114
44	Solutionâ^'Liquidâ^'Solid Growth of Semiconductor Nanowires. Inorganic Chemistry, 2006, 45, 7511-7521.	1.9	321
45	The impact of hyperthermic chemotherapy on human gastric cancer cell lines: preliminary results. Oncology Reports, 2006, 16, 631-41.	1.2	10
46	Benzene Thermal Conversion to Nanocrystalline Indium Nitride from Sulfide at Low Temperature ChemInform, 2003, 34, no.	0.1	0
47	Benzene Thermal Conversion to Nanocrystalline Indium Nitride from Sulfide at Low Temperature. Inorganic Chemistry, 2003, 42, 107-111.	1.9	69
48	Template-based synthesis of nanoscale Ag2E (E = S, Se) dendrites. Journal of Materials Chemistry, 2002, 12, 1148-1151.	6.7	79
49	A mild solvothermal route to chalcopyrite quaternary semiconductor Culn(SexS1 â^ x)2 nanocrystallites. Journal of Materials Chemistry, 2001, 11, 1417-1420.	6.7	79
50	Synthesis and Characterization of Ternary CuInS2 Nanorods via a Hydrothermal Route. Journal of Solid State Chemistry, 2001, 161, 179-183.	1.4	102
51	Novel Ultrasonically Assisted Templated Synthesis of Palladium and Silver Dendritic Nanostructures. Advanced Materials, 2001, 13, 1887.	11.1	235